Available online at www.sciencedirect.com

SciVerse ScienceDirect

Procedia Environmental Sciences 13 (2012) 140 – 150

Procedia Environmental Sciences

The 18th Biennial Conference of International Society for Ecological Modelling

An Improved Algorithm for Forest Fire Detection Using HJ Data

S.D. Wang[a,b*], L.L. Miao[a], G.X. Peng[c]

[a]*College of Resources Science & Technology, Beijing Normal University, Beijing 100875, China*
[b]*School of Surveying and Land Information Engineering, Henan Polytechnic University, Jiaozuo, 454000, China*
[c] *School of Geoscience and Environmental Engineering; Central South University; Changsha, 410083; China*

Abstract

Using the characteristics of the environment and disaster monitoring and forecasting small satellite constellation (HJ), the moderate resolution imaging spectroradiometer (MODIS) forest fire detection contextual algorithm was improved to adapt the HJ-infrared sensor (HJ-IRS). The enhanced method consisted of potential fire pixel identification, absolute and relative fire pixel judgment, background characteristics analysis, and fire pixel confidence. The improved algorithm was programmed in IDL7.1 and tested using HJ forest fire data from Heilongjiang Province in 2009. Results show that improving the forest fire detection contextual algorithm to adapt HJ-IRS is feasible and highly accurate. HJ data are much more sensitive to smaller and cooler fires than MODIS or the advanced very high resolution radiometer (AVHRR) data, and the improved capabilities offers a good potential for application in forest fire detection.

Keywords: MODIS; HJ; forest fire detection; satellite; remote sensing data

* Corresponding author. Tel.: 18910239256; fax: +86-010-58802070.
E-mail address: wsd0908@163.com

 doi:10.1016/j.proenv.2012.01.014

1. Introduction

Forest resources are one of the most important on Earth and the basis of biological diversity. They not only provide a variety of valuable wood and raw materials for production, but also various food for humans. Furthermore, forests can affect the climate by reducing soil erosion and preventing and mitigating drought, wind, and other natural disasters. However, in recent years, many forest fires have broken out in various regions of the world, causing tremendous losses.

Forest fires have been drawing increasing attention in recent years because of their tremendous effect on humans, the environment, wildlife, ecosystem function, weather, and climate. An accurate monitoring and mapping of the spatial and temporal distribution of forest fires is important because it contributes to fire effect assessment and control, as well as to a number of ongoing studies on land use, land cover change, climate change, and so on.

In most cases, a small fire cannot be detected and stopped in time and ultimately leads to a bigger fire. Therefore, an accurate and timely monitoring of forest fires is highly important to protect the ecological environment and forest resources. In the past, forest fire monitoring that relies on manpower and aircraft is costly and inaccurate. However, in recent years, satellite remote sensing technology has become a powerful tool for monitoring forest fires accurately and timely.

Fire detection using satellite data started in the 1980s. A number of scholars at home and abroad conducted research on the methods of forest fire monitoring using different sensors. In general, the National Oceanic and Atmospheric Administration (NOAA) advanced very high resolution radiometer (AVHRR) and moderate resolution imaging spectroradiometer (MODIS) data are used as the main tools in forest fire detection. In recent years, both domestic and foreign researchers developed a variety of forest fire detection algorithms based on remote sensing data, which were tested and applied in the field and exhibited good results. Since the launching of the environment and disaster monitoring and forecasting small satellite constellation (HJ) in China on September 6, 2008, some Chinese scholars tried to use it to monitor forest fires and conducted some preliminary tests. The purpose of this study is to improve existing algorithms and adapt the HJ sensors to promote forest fire monitoring and disaster assessment based on HJ Data.

2. Data and methods

2.1. Existing algorithms

In recent years, a number of researchers have focused on fire detection based on theoretical analysis, the fixed threshold method, or contextual algorithms using NOAA AVHRR multi-channel data. Since the MODIS instruments onboard Terra and Aqua began collecting data in February 2000 and June 2002, respectively, satellite fire detection capability was improved using two 3.96 μm channels [1, 2]. At present, the contextual algorithm is a popular approach to forest fire detection using MODIS data.

The MODIS contextual algorithm consists of three basic parts, namely, preliminary thresholds to identify potential fire pixels, contextual tests to identify fires among the potential fire pixels, and thresholds to reject false alarms [3]. In the first part, the selection of fixed thresholds is subtle as an over-high setting runs the risk of omitting fire pixels [4–10]. Meanwhile, an over-low setting causes more noise in deriving the parameters of the background pixels and generates more false alarms [11–15]. The MODIS version 4 contextual algorithm globally employs fixed thresholds to identify potential fire pixels. For global applications, the preliminary thresholds cannot be set low enough to detect most regional small fires [16–22]. Therefore, it needs improvement for adaptation to fire monitoring and management at the regional scale.

2.2. HJ instrument description

The environment and disaster monitoring and forecasting small satellites HJ-1A and HJ-1B were successfully launched in China on September 6, 2008. The two are optical satellites of the HJ constellation which consists of three satellites [23]. The establishment of the small satellite constellation enables China to monitor disasters and environmental changes more efficiently. The revisit time of the satellite constellation is 48–96 hours.

The two HJ optical satellites provide optical remote sensing information in the visible and infrared spectral bands and can quickly monitor forest fires in a large scale and with multi-spectral resolution [24]. The two small optical satellites can view the entire Earth surface every one to two days. The HJ-1-A satellite carries two CCD cameras and a hyperspectral imager, whereas HJ-1-B carries two CCD cameras and an infrared camera sensor (IRS). The design principles of the four CCD cameras are exactly the same. The cameras are placed symmetrically to the subastral point and divide the field of observation equally, allowing a side-by-side observation and joint pushbroom imaging. The ground swath width of HJ-1A and HJ-1B is 700 km and its ground pixel resolution is 30 m and has four spectral bands. HJ-1-A carries a hyperspectral imager with a 50 km ground swath width. It has a 100 m ground pixel resolution, 110–128 spectral bands, ±30° side observation ability, and a calibration function. The HJ-1-B satellite has an infrared camera, a ground swath width of 720 km, ground pixel resolution of 150 m/300 m, and four spectral bands, namely, near-, short-, mid-, and thermal infrared.

The HJ constellation is a system composed of optical and synthetic aperture radar satellites with high spatial resolution, high time resolution, high spectral resolution, and wide observation width. It can use visible light, infrared, and microwave to meet observation demands for accurate and timely environment monitoring and disaster forecasting.

Based on the advantages of the MODIS algorithm, HJ data are expected to be more sensitive to smaller and cooler fires than MODIS or AVHRR because of their finer spatial resolution. Furthermore, AVHRR/MODIS fire detection algorithms may not be appropriate because of channel differences. Therefore, modifications or new algorithms are necessary.

2.3. Overview of the improved algorithm

2.3.1 Improved algorithm process

Although the infrared bands of HJ-IRS are less than those of MODIS, HJ-IRS has the 4 and 11 μm bands used in detecting forest fires (Table 1). Notwithstanding some differences in subsidiary bands, it can satisfy the requirements of the contextual algorithm based on MODIS. The fire spot detection process of the improved algorithm includes potential fire pixel identification, absolute fire spot judgment, background characteristics analysis, relative fire pixel judgment, and fire pixel confidence. However, this method cannot eliminate false fire pixels because of the difference between HJ and MODIS data. The improved algorithm process is shown in Fig. 1. The specific parameters of each process were adjusted because of the difference between the HJ and MODIS sensors.

Table 1. Comparison of the MODIS and HJ bands used in detecting fire pixels

MODIS				HJ-IRS			
Bands	Center wavelength (μm)	Resolution (m)	Use	Bands	Center wavelength (μm)	Resolution (m)	Use

1	0.65	250	Cloud masking	1(TM4)	0.925	150	Water and cloud masking
2	0.86	250	Cloud masking	2(TM5)	1.65	150	Water and cloud masking
21	4.0	1000	Fire pixel detection				
22	4.0	1000	Fire pixel detection	3(T_4)	3.7	150	Fire pixel detection
31	11.0	1000	Fire pixel detection	4(T_{11})	11.5	300	Fire pixel detection
32	12.0	1000	Cloud masking				

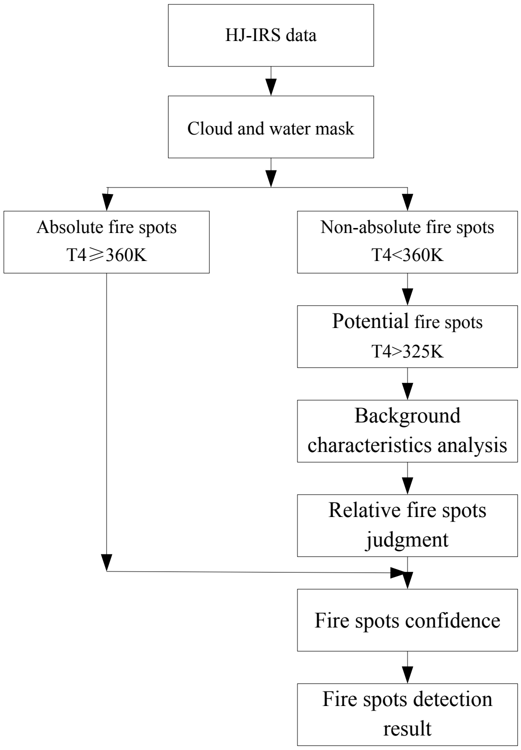

Fig. 1. Fire detection process using HJ-IRS

2.3.2 Water and cloud masking

The MODIS algorithm of forest fire detection extracts water information using MOD03 land and water masking products from MODIS data. Cloud information is extracted from the cloud products by combining several bands based on the cloud detection algorithm. The HJ data products are different from those of MODIS; thus, water and cloud information can only be extracted according to the characteristics of the HJ-IRS data.

(1) Water masking

In general, we can extract water information using the normalized difference water index (NDWI), NDWI = (TM2 - TM5)/ (TM2 + TM5), where TM2 represents the green band and TM5 represents the middle-infrared band. However, we cannot extract water information using NDWI because HJ-IRS lacks the green band. The reflectance of water in the middle-infrared band (1.65 μm) is very low based on the water reflectance spectral curve. Thus, we can extract water information using the middle-infrared band only.

Through statistical analysis, we can derive the judgment condition of water based on the HJ-IRS sensor:

$$Water= (Riance1.65<6) \text{ and } (T4<272\ K) \tag{1}$$

Where, Water refers to water information; Riance1.65 represents the radiation brightness of the infrared band with a 1.65 μm center wavelength; and T4 refers to the brightness temperature of the infrared band with a 4 μm center wavelength.

(2) Cloud masking

The principle of cloud detection is based on the strong reflectivity of the visible light band and the low infrared band temperature. From the cloud detection algorithm based on MODIS data, we perform a statistical analysis of the brightness temperature of the infrared band with an 11 μm center wavelength to obtain the cloud judgment condition based on HJ-IRS, which is shown in the following formula:

$$Cloud= (T11<265) \text{ and } (Water = 0) \tag{2}$$

Where, Cloud refers to cloud information and T11 denotes the brightness temperature of the infrared band with an 11 μm center wavelength.

2.3.3 Detection algorithm components

2.3.3.1 Identification of potential fire pixels

From the statistical analysis, we obtain the judgment threshold value of potential fire pixels at 325 K in the daytime. If the brightness temperature of the third pixel band meets the criterion, T4>325 K, the pixels are considered potential fire pixels.

2.3.3.2 Absolute fire pixel judgment

We use the method of Kaufman to determine the absolute fire pixels. If the brightness temperature of the third band of pixels meets the criterion, T4>360 K, the pixels are considered absolute fire pixels.

2.3.3.3 Background characteristics analysis

We use the adaptive window contextual spatial statistical method to differentiate between the absolute and the potential fire pixels.

Effective background pixels play an important role in spatial statistics, which uses a potential fire pixel as the center. The background pixels should meet the following four conditions: (1) the acquired remote sensing data are not spoiled; (2) the pixels are of land; (3) the pixels are not of cloud; and (4) the pixels are not background fire pixels that meet the T_4>325 K and T_4-T_{11}>20 K requirements. Potential fire pixels are identified by using a potential fire pixel as the center of 5×5, 7×7, and 21×21 size windows. When the number of effective background pixels account for 25% of the total pixels, the search is stopped.

2.3.3.4 Relative fire pixel judgment

After obtaining the effective background pixels, we determine the relative fire pixels using the contextual spatial statistical method. The criteria in the daytime are as follows:

$$[T_4–T_{11}>AVG(T_4–T_{11})+3.5\delta_{(T4–T11)}] \text{ and } [(T_4–T_{11})>AVG(T_4–T_{11}) +6 K] \\ \text{and } [(T_4>AVG(T_4))+3\delta_{(T4)}] \text{ and } \{[T_{11}>AVG_{T11}+\delta_{(T11)} –4 K] \text{ or } [\delta'_{(T4)}>5 K]\} \quad (3)$$

Where, $AVG(T_4–T_{11})$ denotes the mean value of the $T_4–T_{11}$ brightness temperature difference of the effective background pixels; $\delta(T_4–T_{11})$ is the mean absolute deviation of $T_4–T_{11}$; $AVG(T_4)$ refers to the mean value of the T_4 brightness temperature; $AVG(T_{11})$ denotes the mean value of the T_{11} brightness temperature; $\delta(T_4)$ refers to the mean absolute deviation of T_4 of the effective background pixels; $\delta(T_{11})$ denotes the mean absolute deviation of T_{11} of the effective background pixels; and $\delta'(T_4)$ refers to the mean absolute deviation of T4 of the background fire spot pixels.

2.3.3.5 Fire pixel confidence

Confidence is the degree of probability and credibility that the errors between the sampling and the overall pixels do not exceed a certain degree. In this study, we used the Giglio (2003) method to determine the degree of confidence of fire pixel detection. The following parameters were used: T4, representing the 3-band brightness temperature; the brightness temperature difference $\Delta T=T4–T11$ between 3-band and 4-band; 'Naw', the number of water pixels; and 'Nac', the number of cloud pixels among eight that surround each fire pixel when analyzing contextual characteristics. In addition, two variables, Z4 and $Z\Delta T$, are defined as follows:

$$Z_4 = \frac{T_4 - \overline{T_4}}{\delta_4} \quad (4)$$

$$Z_{\Delta T} = \frac{\Delta T - \overline{\Delta T}}{\sigma_{\Delta T}} \quad (5)$$

When calculating for the degree of confidence, the Ramp Function $S(x; \alpha, \beta)$ is denoted as:

$$S(x;\alpha,\beta) = \begin{cases} 0; x \le \alpha \\ (x-\alpha)/(\beta-\alpha); \alpha < x < \beta \\ 1; x \ge \beta \end{cases} \quad (6)$$

daytime: $C_1 = S(T_4; 306K, 340 K)$

night: $C_1 = S(T_4; 302K, 340 K)$ (7)

$$C_2 = S(Z_4; 2.5, 6) \quad (8)$$

$$C_3 = S(Z_{\Delta T}; 3, 6) \quad (9)$$

$$C_4 = 1 - S(Nac;\ 0,\ 6) \tag{10}$$

$$C_5 = 1 - S(Naw;\ 0,\ 6) \tag{11}$$

$$C = \sqrt[5]{C_1 C_2 C_3 C_4 C_5} \tag{12}$$

We can calculate for the degree of confidence of each fire pixel using Formula 9. The degree of confidence ranges from 0 to 1.

3. Results and discussion

The enhanced algorithm was programmed in IDL7.1 and was tested using HJ forest fire data from Heilongjiang Province, Northeast China, in 2009.

The forest fire detection results can be determined using the appropriate judgment rate, which is the percentage of the number of right judgment pixels accounting for the actual fire pixels. In this study, the HJ-CCD burned area pixels in the same region and at the same time were considered as the actual fire pixels of HJ-IRS and MODIS to test the accuracy of forest fire detection.

On April 27, 2009, a forest fire broke out in the Yinanhe Forest in Heilongjiang Province. MODIS passed through the fire area around 11:30 a.m, whereas HJ passed through around 10:30 a.m. The results from HJ-IRS were analyzed using the MODIS fire product data and the burned area images. The spatial resolutions of the MODIS fire products, the burned area images, and the HJ-IRS fire products are 1 km, 30 m, and 150 m, respectively.

For convenient analysis, the 30 m resolution of the HJ-CCD burned area pixels and the 1 km resolution of the MODIS fire products were converted into 150 m. The results of the forest fire detection for the same area at the same time were obtained (Fig. 2 and Table 2).

In Table 2, the IRSCCD and IRSMODIS deviations were calculated using Formulas 10 and 11.

$$\text{IRS}_{\text{CCD}}\text{deviation} = \frac{|\text{IRS fire pixels - CCD}_{150\text{m}}\text{burned area pixels}|}{\text{CCD}_{150\text{m}}\text{burned area pixels}} \times 100\% \tag{13}$$

$$\text{IRS}_{\text{MODIS}}\text{deviation} = \frac{|\text{IRS fire pixels - MODIS}_{150\text{m}}\text{fire pixels}|}{\text{MODIS}_{150\text{m}}\text{fire pixels}} \times 100\% \tag{14}$$

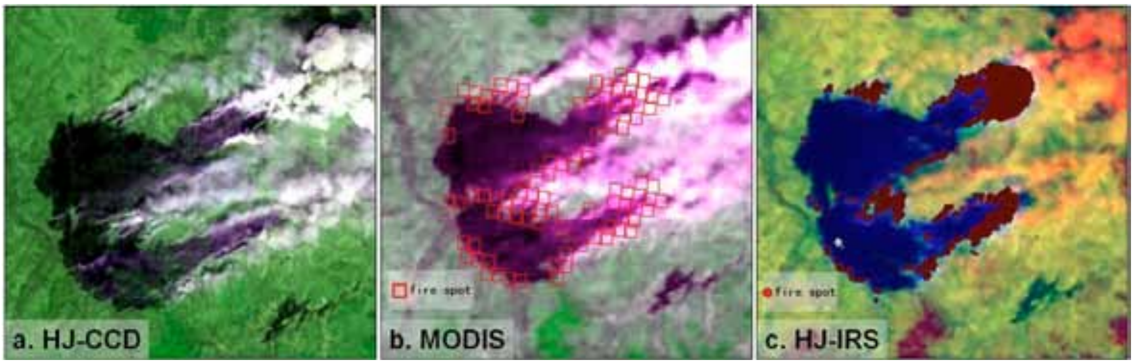

Fig. 2. Fire spot images of the Yinanhe Forest in Heilongjiang Province, April 29, 2009

Table 2. Results of the HJ-IRS, CCD, and MODIS fire pixels

Date	Coordinates of the fire area center (°)	HJ-CCD fire pixels of the burned area	MODIS fire pixels	IRS fire pixels	CCD_{150m} fire pixels of the burned area	$MODIS_{150m}$ fire pixels	IRS_{CCD} deviation (%)	IRS_{MODIS} deviation (%)
April 29	E128.5,N48.6	158628	127	6708	6345	5634	6	19
April 29	E131.0,N47.4	29451	22	1014	1178	976	14	4
April 29	E129.7,N50.9	107492	90	4624	4300	3992	8	16
April 29	E131.7,N49.5	69825	60	3115	2793	2662	12	17
April 29	E134.7,N49.0	7966	6	294	319	266	8	11
May 3	E128.5,N48.6	11222	10	522	449	444	16	18
May 3	E131.0,N47.4	3869	3	142	155	133	8	7
May 3	E128.2,N50.5	3693	3	124	148	133	16	7
May 3	E133.8,N48.1	18882	14	697	755	621	8	12
May 3	E132.7,N48.8	4720	4	212	189	177	12	20
May 19	E101.5,N49.9	7183	6	312	287	266	9	17
May 19	E103.6,N49.8	28120	24	1253	1125	1065	11	18
May 19	E107.3,N49.6	25901	20	906	1036	887	13	2
May 19	E108.5,N49.2	51346	38	1883	2054	1686	8	12
Mean value							11	13

The HJ-CCD burned area pixels at the same time and region were used as the actual HJ-IRS value to test the accuracy of fire pixel detection. The IRSCCD deviation was used to describe the actual accuracy of fire detection using HJ-IRS. Table 2 shows that the IRSCCD deviation ranges from 6% to 14%, with a mean value of 11%. The change is relatively stable, indicating that the improved algorithm based on HJ-IRS is highly accurate. The MODIS fire products at the same time and region were used to test the validity of the fire detection based on HJ-IRS. The IRSMODIS deviation was used to describe the referenced accuracy of fire detection using HJ-IRS. The IRSMODIS deviation ranges from 2% to 19%, with a mean value of 13%. The change is relatively large and unstable, and is attributed to the inherent uncertainties in the MODIS fire products. The 13% mean value of the IRSMODIS deviation also shows that the improved algorithm has high universality and portability. The number of HJ-IRS fire pixels, HJ-CCD burned area pixels, and MODIS fire pixels are shown in Fig. 3. The number of HJ-IRS fire pixels is 23.6 times that of the HJ-CCD fire burned area pixels, which is nearly 25 times that of the theoretically converted value according to the spatial resolution. The degree of similarity, which is defined as the percentage of the two values, is 94%. The number of fire pixels detected by HJ-IRS is 49.9 times that of the number of MODIS fire pixels, which is very close to 44.4 times of the theoretically converted value according to the spatial resolution; the degree of similarity is 89%. The statistical relationship (Fig. 3) further illustrates the feasibility and reliability of the HJ-IRS forest fire detection algorithm.

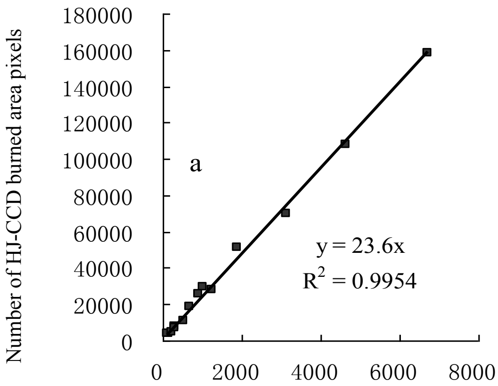

(a) Number of HJ-IRS fire spot pixels

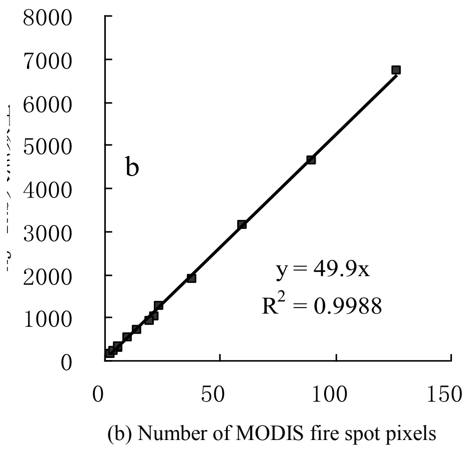

Fig. 3. Scatter diagrams of the HJ-IRS fire pixels, the HJ-CCD burned area pixels, and the MODIS fire pixels

4. Conclusions

The forest fire detection ability of the HJ sensors was evaluated in this study. An improved contextual fire detection algorithm for HJ data was proposed. The work presented in this paper provides both qualitative and quantitative evaluations of a simulated HJ forest fire detection and its characteristics. Several general implications are deduced from this work: (1) On the basis of the MODIS contextual algorithm, the fire detection algorithm based on HJ-IRS was established according to the characteristics of HJ-IRS. (2) The fire detection algorithm was tested and evaluated using the HJ-CCD and MODIS data and images of the burned area at the same time and region. The results show that the mean actual deviation of the burned area was 11%, and the degree of similarity with the number of HJ-CCD fire pixels was 94%. The mean referenced deviation based on the MODIS fire products was 13%, and the degree of similarity with the number of MODIS fire pixels was 89%. Therefore, the improved algorithm is stable and highly reliable. (3) However, the forest fire data used to test and evaluate the algorithm were mainly from Northeast China. The feasibility of the algorithm should be tested at different time intervals and in different regions.

The proposed algorithm is similar to a regional fire detection algorithm because the study area is not large enough. The simulation provides an important method for the evaluation of the HJ fire detection algorithm, but does not completely represent the real landscape. The proposed algorithm must therefore be further tested and evaluated using more HJ data.

Acknowledgements

We appreciate the anonymous reviewers for their constructive comments and suggestions. This study was funded by National Natural Science Foundation of China (41071259), International Scientific and Technological Cooperation Program (2007DFA20640), Beijing Excellent Talents Funding Plan (20081D0503100254) and Beijing Science and Technology New Stars Funding Plan (2008A038).

References

[1] Gao MF, Qin ZH, Liu SC. A Study of Forest Fire Detection Based on MODIS Data. *Remote Sensing for Land & Resources* 2005; **2**:60-3. (in Chinese)

[2] Zhao YS. *Principle and Methods of Remote Sensing Application and Analysis*. Beijing: Science Press; 2003. (in Chinese)

[3] Kaufman YJ, Justice CO, Flynn L P. Potential Global Fire Monitoring from EOS-MODIS. *Journal of Geophysical Research* 1998; **103**: 32215-38.

[4] Dozier JA. Method for Satellite Identification of Surface Temperature Fields of Subpixel Resolution. *Remote Sensing of Environment* 1981; **11**: 221-9.

[5] Qin XJ, Yi HR. A Method to Identify Forest Fire Based on MODIS Data. *Fire Safety Science* 2004; **13**: 83-9. (in Chinese)

[6] Liang Y. Monitoring the Forest Fire by Using EOS/MODIS Data. *Remote Sensing Technology and Application* 2002; **17**: 310-2. (in Chinese)

[7] Liu LM, Yan JJ. Fire Detection Based on EOS MODIS Data. *Geomatics and Information Science of Wuhan University* 2004; **29**: 55-8. (in Chinese)

[8] Zhang SY, Jing YG. Study on Application of EOS-MODIS Data to Forest Fire Monitoring. *Journal of Catastrophology* 2004; **19**: 58-62. (in Chinese)

[9] Zhou XC, Wang XQ. Validation Analysis of the Algorithm for Identifying Forest Fire based on MODIS Data. *Fire Safety Science* 2006; **15**: 31-7. (in Chinese)

[10] Jing H, Xia ZH. The Application of EOS/MODIS Data in Monitor Forest Fire of Hubei Province. *Torrential Rain and Disasters* 2008; **27**: 182-5. (in Chinese)

[11] Peng GX, Shen W, Hu DY. Method to Identify Forest Fire Based on Smoke Plum ES Masking By Using MODIS Data. *J. Infrared Millim*. 2008; **27**:185-9. (in Chinese)

[12] Peng GX, Chen YH, Li J. Combination of Remote Sensing and Meteorological Data for Fire Risk Monitoring-A Case Study in Peninsular Malaysia. *Geo-Information Science* 2007; **9**:99-104. (in Chinese)

[13] Justice C O, Giglio L, Kaufman Y. The MODIS fire products. *Remote Sensing of Environment* 2002; **83**: 244-62.

[14] Giglio L, Descloitres J, Justice CO. An Enhanced Contextual Fire Detection Algorithm for MODIS. *Remote Sensing of Environment* 2003; **87**: 273-82.

[15] Qin XJ, Zhang ZH, Li ZY. An Automatic Forest Fires Identification Method Using HJ-1B IRS Data. *Remote Sensing Technology and Application* 2010; **25**: 700-5. (in Chinese)

[16] Xie QY, Zhang HP, Zhang YM. Experimental study on stokes scattering matrixes of smoke particles. *Infrared Millim. Waves* 2007; **26**: 279-83. (in Chinese)

[17] Xie Y, Qu J, Hao X. Smoke plume detecting using MODIS measurements in eastern United States. East FIRE Conference Proceedings, Fairfax, VA, 2005, May 11-3.

[18] Louis Giglio, Jacques Descloitres. An Enhanced Contextual Fire Detection Algorithm for MODIS. *Remote Sensing of Environment* 2003; **87**: 273-82.

[19] Todd J. Hawbaker, Volker C. Detection rates of the MODIS active fire product in the United States. *Remote Sensing of Environment* 2008; **112**: 2656-64.

[20] Wanting Wang, John J. Qu. An improved algorithm for small and cool fire detection using MODIS data: A preliminary study in the southeastern United States. *Remote Sensing of Environment* 2007; **128**: 163-70.

[21] Wilfrid Schroeder, Elaine Prins. Validation of GOES and MODIS active fire detection products using ASTER and ETM+ data. *Remote Sensing of Environment* 2008; **112**: 2711-26.

[22] Roy DP, Jin Y. Prototyping a global algorithm for systematic fire-affected area mapping using MODIS time series data. *Remote Sensing of Environment* 2005; **97**: 137-62.

[23] Xiang LB, Liu ZH, Wang XB. Hyperspectral Imager of the Environment and Disaster Monitoring Small Satellite. *Remote Sensing Technology and Application* 2009; **24**: 257-62. (in Chinese)

[24] Li SH, Jiao YM. Image Quality Assessment for the HJ-A CCD. *Infrared Technology* 2009; **31**: 167-72. (in Chinese)